International Journal of Dynamics and Control (2026) 14:63
https://doi.org/10.1007/s40435-025-02000-1

$\mathscr{L}_1$-Gain stability analysis for markov jump sampled-data control systems via co-positive-type LKF approach

R. Suresh[1] · G. Devi[2] · R. Vadivel[3] · Nallappan Gunasekaran[4]

Received: 17 May 2025 / Revised: 20 December 2025 / Accepted: 25 December 2025 / Published online: 14 January 2026

Abstract

This study investigates the implementation of sampled-data control techniques in positive Markov jump systems (PMJSs), aiming to ensure exponential stability in the mean and a predefined $\mathscr{L}_1$-gain performance. Initially, we develop a sampled-data model for PMJSs and examine its mean stability characteristics. Subsequently, sufficient criteria are derived to guarantee that the system achieves the targeted $\mathscr{L}_1$-gain performance, with particular emphasis on how the sampling period influences system dynamics. These criteria are utilized to formulate a sampled-data controller, with its gains determined using a linear programming method. The proposed methodology's effectiveness is confirmed through numerical simulations, which support the theoretical results.

Keywords Markovian jump system · sampled-data control · Exponential stability · $\mathscr{L}_1$-gain performance

1 Introduction

Over the past few years, Markov jump systems (MJSs) have attracted significant interest due to their ability to model systems with random switching behaviors [1–6]. These systems are widely applied in diverse domains, including biological modeling, financial systems, networked control, and communication networks, owing to their capacity to handle stochastic dynamics effectively. Traditional analyses of MJSs typically assume continuous state evolution and uninterrupted control inputs [7]. However, the rise of digital technologies has popularized sampled-data control systems, which offer advantages in terms of energy efficiency and reduced hardware costs [8–10]. Consequently, integrating sampled-data control into MJSs, especially positive Markov jump systems (PMJSs), has emerged as a critical research direction. For instance, the authors in [11] discussed the stability and $\mathscr{L}_1$-gain analysis of nonlinear PMJSs with switching transition probabilities, focusing on exponential mean stability and controller synthesis.

PMJSs are distinguished by their non-negative state variables, which enforce positivity constraints on both the system states and outputs. This property makes PMJSs particularly suitable for modeling real-world phenomena, such as traffic flow in communication networks, population dynamics in ecological systems, and disease spread in epidemiological models like the SIS model. Despite these advantages, the positivity requirement poses unique challenges for stability analysis and controller design. In [12] conducted an investigation on the exponential stability and $\mathscr{L}_1$-gain performance of positive time delay Markov jump systems (MJSs) with switching transition rates. The findings of this study provide valuable insights into the management of delays in such systems. In a similar manner, [13] conducted an analysis on the stability and $\mathscr{L}_1$-gain performance of positive switched systems that included mixed time-varying delays. They pre-

✉ R. Suresh
sureshsiththan@gmail.com

✉ R. Vadivel
vadivelsr@yahoo.com

G. Devi
devi.maths@sairam.edu.in

Nallappan Gunasekaran
gunasmaths@gmail.com

[1] Department of Mathematics, Sri Venkateswara College of Engineering, Sriperumbudur 602117, TamilNadu, India

[2] Department of Mathematics, Sri Sai Ram Engineering College, Chennai 600044, TamilNadu, India

[3] Department of Mathematics, Faculty of Science and Technology, Phuket Rajabhat University, Phuket 83000, Thailand

[4] Eastern Michigan Joint College of Engineering, Beibu Gulf University, Qinzhou 535011, Guangxi, China

sented adequate requirements to guarantee both stability and the required performance. Additionally, [14, 15] constructed a state feedback controller by employing linear programming techniques. These researchers established necessary and sufficient criteria for the stochastic stability of PMJLSs.

An essential component of evaluating PMJSs is the formulation of suitable Lyapunov–Krasovskii functionals (LKFs). Although conventional positive Lyapunov–Krasovskii functionals (LKFs) have been utilized for positive systems, the co-positive-type LKF methodology has unique benefits for positive Markov jump systems (PMJSs). Co-positive LKFs provide the integration of both present state data and previous state trajectories via integral terms, while preserving the positivity restriction across the functional. This attribute is especially significant for sampled-data control systems, because the delay caused by sampling $\hbar(t)$ necessitates meticulous consideration of state history. The co-positive structure facilitates the derivation of stability criteria by leveraging the interaction between positive states and positive weighting vectors, which is especially helpful in addressing the sampling-induced delay $\hbar(t)$ within the positivity framework.

Sampled-data control systems are important in digital control applications and have been extensively studied. For efficient processing and control, these systems transform continuous signals into discrete data. Their work addresses sampling and discretization issues while preserving stability and performance. The authors in [16] outlined key approaches for analyzing sampled-data systems, including the direct design method, which relies on an accurate sampled-data model to meet stability and performance goals without approximations. This method, while complex, ensures robust stability and performance, making it a preferred choice for precise control design. The significance of sampled-data control has led to numerous studies in this area. For example, in [17], Zhang and Li conducted a study on the exponential stability and $\mathscr{L}_1$ -gain properties of positive sampled-data systems in a deterministic context, excluding random phenomena, which differs from the stochastic nature of PMJSs. The authors in [18] proposed a novel sampling sequence that combines varying intervals to achieve global exponential stability, effectively addressing challenges posed by large sampling intervals.

This paper suggests a substantial contribution by broadening sampled-data control techniques to PMJSs and offering a detailed analysis of their exponential stability in the mean and $\mathscr{L}_1$-gain performance. In addition, this study provides a set of findings that are notable in nature. This begins with the formulation of a sampled-data model for PMJSs, followed by an investigation into the mean exponential stability of the model. After that, enough conditions are provided to guarantee exponential stability while also assuring a weighted $\mathscr{L}_1$-gain attribute. This enhances the system's robustness when it comes to Markovian mode transitions. In conclusion, a sampled-data controller is developed with the purpose of preserving the positivity of the system while simultaneously meeting the stability and effectiveness criteria that are demanded. The controller gains are computed using a linear programming approach, and the theoretical results are validated through numerical examples.

Table 1 Notations used in this paper

Notation	Description
$\mathbb{R}^n$	n-dimensional Euclidean space
$\mathbb{R}^{n\times m}$	$n \times m$ real matrices
$\|\|x\|\|$	Euclidean norm in $\mathbb{R}^n$
A^T	Transpose of a matrix A
$E\{x\}$	Expectation of a random variable x

The paper is organized as follows. The problem formulation, PMJS model with sampled-data control, and key definitions and lemmas are presented in Sect. 2 . Section 3 is the main contribution of this work, where Sect. 3.1 establishes sufficient conditions for exponential mean stability using Theorem 1, Sect. 3.2 derives $\mathscr{L}_1$-gain performance criteria using Theorem 2, and sect. 3.3 presents the linear programming controller design methodology in Theorem 3. Section 4 provides two detailed numerical examples to support the theoretical conclusions and prove that the technique works. Section 5 closes the work and suggests future research.

Table 1 lists the main mathematical notations used in this study. These control systems literature notations will be applied consistently in the study. In particular, $\mathbb{R}^n$ represents the state space for the system (1) and $\mathbb{R}^{n\times m}$ represents the space of real matrices used for system matrices (e.g., $\mathfrak{G}_{0i}$, $\mathfrak{G}_{1i}$). The Euclidean norm $||x||$ and expectation operator E. are crucial for establishing exponential stability in 2 and $\mathscr{L}_1$-gain performance in 3.

2 Problem formulation and preliminaries

We examine a class of PMJSs described by the following dynamics:

$$\begin{aligned}\dot{\xi}(t) &= \mathfrak{G}_0(\Upsilon(t))\xi(t) + \mathfrak{G}_1(\Upsilon(t))\xi(t-\nu(t)) \\ &\quad + \mathfrak{G}_3(\Upsilon(t))\hat{u}(t) + \mathfrak{G}_2(\Upsilon(t))\hat{w}(t), \\ \hat{z}(t) &= \mathfrak{H}_0(\Upsilon(t))\xi(t) + \mathfrak{H}_1(\Upsilon(t))\hat{w}(t),\end{aligned} \tag{1}$$

where $\xi(t) \in \mathbb{R}^n$ represents the system state, $\hat{z}(t) \in \mathbb{R}^{n_{\hat{z}}}$ is the output, $\hat{w}(t) \in \mathbb{R}^{n_{\hat{w}}}$ denotes the disturbance input belonging to $\mathscr{L}_1[0,\infty)$, and and $\hat{u}(t) \in \mathbb{R}^{n_{\hat{u}}}$ serves as the control input. The delay $\nu(t)$ satisfies $\nu(t) \in [0, \nu]$ with its derivative

$\dot{\nu}(t) = \nu_0$. The mode transitions are governed by the Markov process $\Upsilon(t) : [0, \infty) \to \mathscr{Q} = 1, 2, ..., N$ with transition probabilities defined as:

$$Pr(\Upsilon(t+\Delta) = j|\Upsilon(t) = i) = \begin{cases} \pi_{i,j}\Delta + o(\Delta), & i \neq j; \\ 1 + \pi_{i,i}\Delta + o(\Delta), & i = j, \end{cases}$$

where $\pi_{i,j} \geq 0$ represents the transition rate from mode i to mode j $(i \neq j)$, $\pi_{i,i} = -\sum_{j=1,j\neq i}^{N} \pi_{i,j}$ and $\Delta > 0$. The transition rate matrix is defined as $\Pi = (\pi_{i,j})_{n\times n}$. For a given mode $\Upsilon(t) = i \in \mathscr{Q}$, the system matrices $\mathfrak{G}_0(\Upsilon(t))$, $\mathfrak{G}_1(\Upsilon(t))$, $\mathfrak{G}_2(\Upsilon(t))$, $\mathfrak{H}_0(\Upsilon(t))$ and $\mathfrak{H}_1(\Upsilon(t))$ are denoted by $\mathfrak{G}_{0i}, \mathfrak{G}_{1i}, \mathfrak{G}_{2i}, \mathfrak{H}_{0i}$ and $\mathfrak{H}_{1i}$, respectively, and are constant matrices of suitable dimensions. The state at time t, denoted by $\xi(t, x_0, \Upsilon_0)$, corresponds to the initial conditions at $t_0 = 0$, with initial state $\xi(0) = (\xi_{01}, ..., \xi_{0n})^T$ and initial mode $\Upsilon(0) = \Upsilon_0$. For simplicity, $\xi(t)$ is used in place of $\xi(t, x_0, \Upsilon_0)$ when the context is clear. It is assumed that the state $\xi(t)$ does not exhibit jumps at the instants of mode switching.

Definition 1 [19] System (1) is considered to be positive if, for any initial state that satisfies the condition $\xi_0 \geq 0$, when a non-negative disturbance $\hat{w}(t) \geq 0$ and a control input $\hat{u}(t) \geq 0$ are present, the resulting state trajectory remains non-negative, meaning that $\xi(t) \geq 0$ and $\hat{z}(t) \geq 0$ for all $t \geq 0$.

A matrix $\mathfrak{G}_0 \in \mathbb{R}^{n\times n}$ is termed a Metzler matrix when all its off-diagonal elements are non-negative. According to established results ([20], [21]), system (1) exhibits positivity if and only if, for each mode $i \in \mathscr{Q}$, the matrix $\mathfrak{G}_{0i}$ is Metzler and $\mathfrak{G}_{2i} \in R_+^{n\times n_{\hat{w}}}$

Remark 1 To guarantee the system's positivity, the Metzler matrix property of $\mathfrak{G}_{0i}$ is essential. If every off-diagonal element in a matrix is non-negative, the matrix is said to be Metzler. This characteristic ensures that the state derivative $\xi(t)$ does not result in any state component becoming negative because of interactions between various state variables when $\xi(t) \geq 0$. In particular, for the continuous-time positive system (1), if $\xi(t) \geq 0$ and $\mathfrak{G}_{0i}$ is Metzler, then the diagonal elements (which may be negative) regulate the decay rate of individual states, while the coupling terms between states (off-diagonal elements of $\mathfrak{G}_{0i}\xi(t)$) remain non-negative.

Definition 2 [12]The system (1) with the value of $\hat{w}(t) = 0$ and $\hat{u}(t) = 0$ is claimed that is exponentially stable in the mean if the condition is fulfilled by its solution $\xi(t)$.

$$\mathbb{E}\{\|\xi(t)\|\} \leq \beta\|\xi_0\|e^{-\rho(t-t_0)}, \forall t \geq t_0,$$

where β and ρ are positive constants.

Definition 3 [13] In the presence of positive scalars ρ and γ, the system (1) with $\hat{u}(t) = 0$ is regarded to have achieved a predetermined $\mathscr{L}_1$-gain performance level γ if the requirements listed below are met:

(a) When $\hat{w}(t) = 0$, the system (1) demonstrates exponential stability in the mean and demonstrates this stability.
(b) Assuming that the starting state of the system is zero $(\xi_0 = 0)$, the system (1) is able to satisfy the following inequality

$$\mathbb{E}\left\{\int_{\infty}^{t_0} e^{-\rho(t-t_0)}\|\hat{z}(t)\|_1\, dt\right\} \leq \gamma\mathbb{E}\left\{\int_{\infty}^{t_0} \|\hat{w}(t)\|_1\}dt\right\}, \text{ for } \hat{w}(t) \neq 0.$$

Remark 2 The idea presented in [13] is expanded upon in Definition 3, which incorporates stochastic systems within its scope. The efficient functioning of the system is characterized by the $\mathscr{L}_1$-gain, which indicates its capacity to lessen the effect of external disturbances. A smaller γ indicates superior performance, meaning the disturbance input has a reduced influence on the controlled output.

The zero-order hold (ZOH) mechanism in system (1) generates the control signals $\hat{u}(t)$. Through sampling at predetermined intervals, this method discretizes the continuous-time system. These sampling instants form an increasing sequence of time points $0 = t_0 < t_1 < t_2 < \cdots < t_k < \ldots$, where t_k represents the k-th sampling instant. The value of the system state $\xi(t_k)$ at every given sampling time t_k determines the control signal, which stays constant for the length of the period $[t_k, t_{k+1})$. Then provides the control signal for this interval:

$$\hat{u}(t) = \mathscr{K}_i\xi(t_k), \quad \text{for } t_k \leq t < t_{k+1}, \tag{2}$$

where $\mathscr{K}_i$ denotes the control law applied during the interval, based on the system state at time t_k. Under the assumption that $\lim_{k\to\infty} t_k = \infty$, the sampling series will go on forever. Furthermore, the sampling interval is limited such that, for every $k \geq 0$, where $\hbar$ is a positive constant, the time difference between successive sampling points fulfills $t_{k+1} - t_k \leq \hbar$.

The objective of this study is to design a sampled-data controller that guarantees the closed-loop system's positivity, mean exponential stability, and a desired $\mathscr{L}_1$ - gain performance. Using a method similar to that in [22], we represent the sampling time as $t_k = t - \hbar(t)$, where $\hbar(t) = t - t_k$. This allows us to view the digital control as a continuous controller with a time-varying delay. As a result, system (1) can be re-expressed as a time delay PMJLS

$$\dot{\xi}(t) = \mathfrak{G}_{0i}\xi(t) + \mathfrak{G}_{1i}\xi(t - \nu(t)) + \mathfrak{G}_{2i}\hat{w}(t)$$

$$+ \mathfrak{G}_{3i}\mathscr{K}_i\xi(t-\hbar(t)),$$
$$\hat{z}(t) = \mathfrak{H}_{0i}\xi(t) + \mathfrak{H}_{1i}\hat{w}(t), \tag{3}$$

where $\hbar(t) \in [0, \hbar]$ and $\dot{\hbar}(t) = 1$ for $t \neq t_k$.

Lemma 1 *[23] It is assumed that the system (3) demonstrates positivity if and only if, for any mode i that belongs to the set $\mathscr{Q}$, the matrix $\mathfrak{G}_{0i}$ is a Metzler matrix, and the subsequent requirements hold:*

1. $\mathfrak{G}_{2i} \in \mathbb{R}_+^{n\times n_{\hat{w}}}$,
2. $\mathfrak{G}_{3i}\mathscr{K}_i \in \mathbb{R}_+^{n\times n_{\hat{u}}}$,
3. $\mathfrak{H}_{0i} \in \mathbb{R}_+^{n_{\hat{z}}\times n}$,
4. $\mathfrak{H}_{1i} \in \mathbb{R}_+^{n_{\hat{z}}\times n_{\hat{w}}}$.

Remark 3 The authors of the study [24] examined a stability analysis and the design of an $\mathscr{L}_1$-gain controller for a class of switched positive T-S fuzzy systems with time-varying delays. When compared to the controller techniques in the above paper, sampled-data control has been utilized in this work to check the exponentially stable conditions.

3 Main results

This section presents an analysis of exponential stability, $\mathscr{L}_1$ - gain performance and control synthesis for the time delay PMJLS (3).

3.1 Stability analysis

By using a positive Lyapunov–Krasovskii functional (LKF), we establish conditions for the mean exponential stability of the closed-loop system (3) when $\hat{w}(t) = 0$. These conditions are presented in the theorem below.

Theorem 1 *For a given scalar $\rho > 0$, the positive system (3 with $\hat{w}(t) = 0$ is exponentially stable in the mean if there exists vectors $v_i, \varsigma_{1,i}, \varsigma_{2,i}, \varsigma_{3,i}, \varsigma_{4,i}, \varsigma_1, \varsigma_2, \varsigma_3, \varsigma_4 \in \mathbb{R}_+^n$ for all $(i \in S)$, satisfying the inequalities:*

$$\mathfrak{G}_{0i}^T v_i + \rho v_i + \varsigma_{1,i} + \varsigma_{2,i} + \varsigma_{3,i} + \varsigma_{4,i} + \nu\varsigma_1 + \nu\varsigma_2 + \hbar\varsigma_3 + \hbar\varsigma_4 + \sum_{j=1}^{N}\pi_{ij}v_j < 0, \tag{4}$$

$$\mathfrak{G}_{1i}^T v_i - \mathfrak{U}\varsigma_{1,i} - \mathfrak{T}\varsigma_{2,i} < 0, \tag{5}$$

$$\mathscr{K}_i^T\mathfrak{G}_{3i}^T v_i - \mathfrak{V}\varsigma_{4,i} < 0, \tag{6}$$

where

$$\sum_{j=1}^{N}\pi_{ij}\varsigma_{1,j} \le \varsigma_1, \sum_{j=1}^{N}\pi_{ij}\varsigma_{2,j} \le \varsigma_2, \sum_{j=1}^{N}\pi_{ij}\varsigma_{3,j} \le \varsigma_3, \sum_{j=1}^{N}\pi_{ij}\varsigma_{4,j} \le \varsigma_4, \tag{7}$$

$\mathfrak{T} = e^{-\rho\nu}, \mathfrak{U} = (1-\nu_0)\mathfrak{T}, \mathfrak{V} = e^{-\rho\hbar}$.

Proof Construct a co-positive-type LKF candidate as:

$$V(t,\xi(t),i) = \sum_{r=1}^{5} V_r(t,\xi(t),i), \tag{8}$$

where

$$V_1(t,\xi(t),i) = \xi^T(t)v_i,$$
$$V_2(t,\xi(t),i) = \int_{t-\nu(t)}^{t} e^{\rho(s-t)}\xi^T(s)\varsigma_{1,i}ds + \int_{t-\nu}^{t} e^{\rho(s-t)}\xi^T(s)\varsigma_{2,i}ds,$$
$$V_3(t,\xi(t),i) = \int_{t-\hbar(t)}^{t} e^{\rho(s-t)}\xi^T(s)\varsigma_{3,i}ds + \int_{t-\hbar}^{t} e^{\rho(s-t)}\xi^T(s)\varsigma_{4,i}ds,$$
$$V_4(t,\xi(t),i) = \int_{-\nu}^{0}\int_{t+\theta}^{t} e^{\rho(s-t)}\xi^T(s)(\varsigma_1+\varsigma_2)dsd\theta$$
$$V_5(t,\xi(t),i) = \int_{-\hbar}^{0}\int_{t+\theta}^{t} e^{\rho(s-t)}\xi^T(s)(\varsigma_3+\varsigma_4)dsd\theta,$$

with $v_i, \varsigma_{1,i}, \varsigma_{2,i}, \varsigma_{3,i}, \varsigma_{4,i}, \varsigma_1, \varsigma_2, \varsigma_3, \varsigma_4 \in \mathbb{R}_+^n$, and satisfying:

$$\sum_{j=1}^{N}\pi_{ij}\varsigma_{1,j} \le \varsigma_1, \sum_{j=1}^{N}\pi_{ij}\varsigma_{2,j} \le \varsigma_2, \sum_{j=1}^{N}\pi_{ij}\varsigma_{3,j} \le \varsigma_3, \sum_{j=1}^{N}\pi_{ij}\varsigma_{4,j} \le \varsigma_4.$$

We compute the infinitesimal operator $\mathscr{L}$ acting on $V(t,\xi(t),i)$ along the trajectories of system (3):

$$\begin{aligned}\mathscr{L}V(t,\xi(t),i) &= \xi^T(t)[\mathfrak{G}_{0i}^T v_i + \rho v_i + \varsigma_{1,i} + \varsigma_{2,i} + \varsigma_{3,i} + \varsigma_{4,i} \\ &+ \nu\varsigma_1 + \nu\varsigma_2 + \hbar\varsigma_3 + \hbar\varsigma_4 + \sum_{j=1}^{N}\pi_{ij}v_j] \\ &+ \xi^T(t-\nu(t))\mathfrak{G}_{1i}^T v_i - (1-\dot{\nu}(t))e^{-\rho\nu(t)}\xi^T(t-\nu(t))\varsigma_{1,i} \\ &- e^{-\rho\nu}\xi^T(t-\nu)\varsigma_{2,i} + \xi^T(t-\hbar(t))\mathscr{K}_i^T\mathfrak{G}_{3i}^T v_i \\ &- (1-\dot{\hbar}(t))e^{-\rho\hbar(t)}\xi^T(t-\hbar(t))\varsigma_{3,i} \\ &- e^{-\rho\hbar}\xi^T(t-\hbar)\varsigma_{4,i}\end{aligned}$$

$$+\sum_{j=1}^{N}\pi_{ij}\int_{t-\nu(t)}^{t}e^{\rho(s-t)}\xi^T(s)\varsigma_{1,j}ds$$
$$+\sum_{j=1}^{N}\pi_{ij}\int_{t-\nu}^{t}e^{\rho(s-t)}\xi^T(s)\varsigma_{2,j}ds$$
$$-\int_{t-\nu}^{t}e^{\rho(s-t)}\xi^T(s)(\varsigma_1+\varsigma_2)ds$$
$$+\sum_{j=1}^{N}\pi_{ij}\int_{t-\hbar(t)}^{t}e^{\rho(s-t)}\xi^T(s)\varsigma_{3,j}ds$$
$$+\sum_{j=1}^{N}\pi_{ij}\int_{t-\hbar}^{t}e^{\rho(s-t)}\xi^T(s)\varsigma_{4,j}ds$$
$$-\int_{t-\hbar}^{t}e^{\rho(s-t)}\xi^T(s)(\varsigma_3+\varsigma_4)ds-\rho V(t,\xi(t),i).$$

Using the constraint in (7), this simplifies to:

$$\begin{aligned}&\mathscr{L}V(t,\xi(t),i)\\&=\xi^T(t)[\mathfrak{G}_{0i}^Tv_i+\rho v_i+\varsigma_{1,i}+\varsigma_{2,i}+\varsigma_{3,i}+\varsigma_{4,i}\\&+\nu\varsigma_1+\nu\varsigma_2+\hbar\varsigma_3+\hbar\varsigma_4+\sum_{j=1}^{N}\pi_{ij}v_j]\\&+\xi^T(t-\nu(t))\mathfrak{G}_{1i}^Tv_i-(1-\dot{\nu}(t))e^{-\rho\nu(t)}\xi^T(t-\nu(t))\varsigma_{1,i}\\&-e^{-\rho\nu}\xi^T(t-\nu)\varsigma_{2,i}+\xi^T(t-\hbar(t))\mathscr{K}_i^T\mathfrak{G}_{3i}^Tv_i\\&-(1-\dot{\hbar}(t))e^{-\rho\hbar(t)}\xi^T(t-\hbar(t))\varsigma_{3,i}\\&-e^{-\rho\hbar}\xi^T(t-\hbar)\varsigma_{4,i}-\rho V(t,\xi(t),i).\end{aligned}$$

Employing inequalities (4)- (6), we obtain,

$$\mathscr{L}V(t,\xi(t),i)\le-\rho V(t,\xi(t),i). \tag{9}$$

Following the methodology of Theorem 1 in [25], which utilizes Dynkin's formula and the Gronwall–Bellman lemma, we derive the following inequality for $t\ge t_0$.

$$E\{V(t,\xi(t),\Upsilon(t))|\xi_0,\Upsilon_0\}\le e^{-\rho(t-t_0)}V(t_0,\xi(t_0),\Upsilon_0). \tag{10}$$

Defining $p_1=\min_{(i,j)\in P\times I_n}\{v_{ij}\}$, $p_2=\max_{(i,j)\in P\times I_n}\{v_{ij}\}$, $p_3=\max_{(i,j)\in P\times I_n}\{\varsigma_{1,ij}\}$, $p_4=\max_{(i,j)\in P\times I_n}\{\varsigma_{2,ij}\}$, $p_5=\max_{(i,j)\in P\times I_n}\{\varsigma_{3,ij}\}$, $p_6=\max_{(i,j)\in P\times I_n}\{\varsigma_{4,ij}\}$, $p_7=\max_{(i,j)\in P\times I_n}\{\varsigma_{1,j}\}$, $p_8=\max_{(i,j)\in P\times I_n}\{\varsigma_{2,j}\}$, $p_9=\max_{(i,j)\in P\times I_n}\{\varsigma_{3,j}\}$ and $p_{10}=\max_{(i,j)\in P\times I_n}\{\varsigma_{4,j}\}$, the following bounds hold:

$$V(t,\xi(t),i)\ge p_1\|\xi(t)\|, \tag{11}$$

$$\begin{aligned}&V(t_0,\xi_0,\Upsilon_0)\\&\le p_2\|\xi_0\|+p_3\int_{t_0-\nu(t_0)}^{t_0}e^{\rho(s-t_0)}\|\xi_0\|ds\\&+p_4\int_{t_0-\nu}^{t_0}e^{\rho(s-t_0)}\|\xi_0\|ds\\&+p_5\int_{t_0-\hbar(t_0)}^{t_0}e^{\rho(s-t_0)}\|\xi_0\|ds+p_6\int_{t_0-\hbar}^{t_0}e^{\rho(s-t_0)}\|\xi_0\|ds\\&+(p_7+p_8)\int_{-\nu}^{0}\int_{t_0+\theta}^{t_0}e^{\rho(s-t_0)}\|\xi_0\|dsd\theta\\&+(p_9+p_{10})\int_{-\hbar}^{0}\int_{t_0+\theta}^{t_0}e^{\rho(s-t_0)}\|\xi_0\|dsd\theta\\&\le\Bigg[p_2+(p_3+p_4)\frac{\nu}{\rho}(1-e^{-\rho\nu})+(p_5+p_6)\frac{\hbar}{\rho}(1-e^{-\rho\hbar})\\&+(p_7+p_8)\frac{1}{\rho}\left(\nu-\frac{1}{\rho}+\frac{e^{-\rho\nu}}{\rho}\right)\\&+(p_9+p_{10})\frac{1}{\rho}\left(\hbar-\frac{1}{\rho}+\frac{e^{-\rho\hbar}}{\rho}\right)\Bigg]\|\xi_0\|\end{aligned} \tag{12}$$

Combining (10)-(12), we get

$$E[\|\xi(t)\|]\le\tilde{\alpha}e^{-\rho(t-t_0)}\|\xi_0\|,$$

where

$$\tilde{\alpha}=\frac{p_2+(p_3+p_4)\frac{\nu}{\rho}(1-e^{-\rho\nu})+(p_5+p_6)\frac{\hbar}{\rho}(1-e^{-\rho\hbar})+(p_7+p_8)\frac{1}{\rho}(\nu-\frac{1}{\rho}+\frac{e^{-\rho\nu}}{\rho})+(p_9+p_{10})\frac{1}{\rho}(\hbar-\frac{1}{\rho}+\frac{e^{-\rho\hbar}}{\rho})}{p_1}.$$

Thus, if inequalities (4)-(7) are satisfied, system (3) is exponentially stable.

Remark 4 Theorem 1 indicates, through inequality (4), that the maximum sampling period $\hbar$ influences the existence and values of v_i, thereby impacting the system's stability.

3.2 $\mathscr{L}_1$ -gain performance analysis

The following theorem provides sufficient conditions for the positive system (3) to achieve exponential stability while satisfying a weighted $\mathscr{L}_1$- gain property.

Theorem 2 *For a scalar $\rho>0$, the system (3) is considered to attain a designated $\mathscr{L}_1$-gain performance level $\gamma>0$ if there exist some vectors $v_i,\varsigma_{1,i},\varsigma_{2,i},\varsigma_{3,i},\varsigma_{4,i},\varsigma_1,\varsigma_2,\varsigma_3,\varsigma_4\in\mathbb{R}_+^n$ for all $(i\in S)$, satisfying*

$$\mathfrak{G}_{0i}^Tv_i+\rho v_i+\varsigma_{1,i}+\varsigma_{2,i}+\varsigma_{3,i}+\varsigma_{4,i}$$

$$+ \nu\varsigma_1 + \nu\varsigma_2 + \hbar\varsigma_3 + \hbar\varsigma_4 + \sum_{j=1}^{N} \pi_{ij} v_j + \mathfrak{H}_{0i}^T \mathbf{1} < 0, \tag{13}$$

$$\mathfrak{G}_{1i}^T v_i - \mathfrak{U}\varsigma_{1,i} - \mathfrak{T}\varsigma_{2,i} < 0, \tag{14}$$

$$\mathscr{K}_i^T \mathfrak{G}_{3i}^T v_i - \mathfrak{V}\varsigma_{4,i} < 0, \tag{15}$$

$$\mathfrak{G}_{2i}^T v_i + \mathfrak{H}_{1i}^T \mathbf{1} - \gamma \mathbf{1} < 0, \tag{16}$$

where

$$\sum_{j=1}^{N} \pi_{ij}\varsigma_{1,j} \le \varsigma_1, \sum_{j=1}^{N} \pi_{ij}\varsigma_{2,j} \le \varsigma_2, \sum_{j=1}^{N} \pi_{ij}\varsigma_{3,j} \le \varsigma_3, \sum_{j=1}^{N} \pi_{ij}\varsigma_{4,j} \le \varsigma_4, \tag{17}$$
$$\mathfrak{T} = e^{-\rho\nu}, \mathfrak{U} = (1-\nu_0)\mathfrak{T}, \mathfrak{V} = e^{-\rho\hbar}.$$

Proof According to Theorem 1, the mean exponential stability of (3) with $\hat{w}(t) = 0$ is guaranteed if the inequalities (4) through (7) are valid. For the purpose of demonstrating the $\mathscr{L}_1$-gain performance of the system (3), we include the identical co-positive LKF candidate that was used in (8):

$$\begin{aligned}
&\mathscr{L}V(t,\xi(t),i) + \|\hat{z}(t)\|_1 - \gamma\|\hat{w}(t)\|_1 \\
&= \xi^T(t)[\mathfrak{G}_{0i}^T v_i + \rho v_i + \varsigma_{1,i} + \varsigma_{2,i} + \varsigma_{3,i} + \varsigma_{4,i} \\
&+ \nu\varsigma_1 + \nu\varsigma_2 + \hbar\varsigma_3 + \hbar\varsigma_4 + \sum_{j=1}^{N} \pi_{ij} v_j + \mathfrak{H}_{0i}^T \mathbf{1}] \\
&+ \xi^T(t-\nu(t))\mathfrak{G}_{1i}^T v_i - (1-\dot{\nu}(t))e^{-\rho\nu(t)}\xi^T(t-\nu(t))\varsigma_{1,i} \\
&- e^{-\rho\nu}\xi^T(t-\nu)\varsigma_{2,i} + \xi^T(t-\hbar(t))\mathscr{K}_i^T\mathfrak{G}_{3i}^T v_i \\
&- (1-\dot{\hbar}(t))e^{-\rho\hbar(t)}\xi^T(t-\hbar(t))\varsigma_{3,i} \\
&- e^{-\rho\hbar}\xi^T(t-\hbar)\varsigma_{4,i} \\
&+ \hat{w}^T(t)(\mathfrak{G}_{2i}^T v_i + \mathfrak{H}_{1i}^T\mathbf{1} - \gamma\mathbf{1}) - \rho V(t,\xi(t),i).
\end{aligned}$$

Taking into consideration the stated initial conditions (zero), the ensuing inequalities (13)-(17) guarantee that

$$\mathscr{L}V(t,\xi(t),i) + \|\hat{z}(t)\|_1 - \gamma\|\hat{w}(t)\|_1 < 0.$$

Using Dynkin's formula, we have shown that under circumstances of initial conditions (zero),

$$\begin{aligned}
E\left\{\int_{t_0}^{t} \mathscr{L}V(t,\xi(t),i)\right\} &= E\{V(t,\xi(t),i)\} - E\{V(t_0,\xi_0,\Upsilon_0)\} \\
&= E\{V(t,\xi(t),i).
\end{aligned}$$

Thus,

$$\begin{aligned}
&E\left\{\int_{t_0}^{t} \|\hat{z}(t)\|_1 - \gamma\|\hat{w}(t)\|_1 dt\right\} \\
&= E\left\{\int_{t_0}^{t} \|\hat{z}(t)\|_1 - \gamma\|\hat{w}(t)\|_1 dt + \mathscr{L}V(t,\xi(t),i)\right\} \\
&- E\left\{\int_{t_0}^{t} \mathscr{L}V(t,\xi(t),i)\right\} \\
&= E\left\{\int_{t_0}^{t} \|\hat{z}(t)\|_1 - \gamma\|\hat{w}(t)\|_1 dt + \mathscr{L}V(t,\xi(t),i)\right\} \\
&- E\{V(t,\xi(t),i)\} \\
&\le E\left\{\int_{t_0}^{t} \|\hat{z}(t)\|_1 - \gamma\|\hat{w}(t)\|_1 dt + \mathscr{L}V(t,\xi(t),i)\right\} \\
&- E\{V(t,\xi(t)\} < 0.
\end{aligned}$$

This implies

$$\begin{aligned}
E\left\{\int_{t_0}^{\infty} \|\hat{z}(t)\|_1 dt\right\} &= \lim_{t\to\infty} E\left\{\int_{t_0}^{\infty} \|\hat{z}(t)\|_1 dt | (\xi_0, \Upsilon_0)\right\} \\
&\le \gamma E\left\{\int_{t_0}^{\infty} \|\hat{w}(t)\|_1 dt\right\},
\end{aligned}$$

that the $\mathscr{L}_1$-gain performance has been achieved. As a result, the system (3) is able to achieve the desired $\mathscr{L}_1$-gain performance level, which is $\gamma > 0$.

3.3 Controller design

In this particular section, our primary purpose is to create a sampled-data controller (2) that not only assures exponential stability but also guarantees a weighted $\mathscr{L}_1$-gain for the system (3). The most important findings on the controller design are summarized in the following theorem.

Theorem 3 *For a known scalar $\rho > 0$, if there exist vectors, $v_i, \varsigma_{1,i}, \varsigma_{2,i}, \varsigma_{3,i}, \varsigma_{4,i}, z_i, \varsigma_1, \varsigma_2, \varsigma_3, \varsigma_4 \in \mathbb{R}_+^n (i \in S)$ satisfying*

$$\begin{aligned}
&\mathfrak{G}_{0i}^T v_i + \rho v_i + \varsigma_{1,i} + \varsigma_{2,i} + \varsigma_{3,i} + \varsigma_{4,i} \\
&+ \nu\varsigma_1 + \nu\varsigma_2 + \hbar\varsigma_3 + \hbar\varsigma_4 + \sum_{j=1}^{N} \pi_{ij} v_j + \mathfrak{H}_{0i}^T \mathbf{1} < 0,
\end{aligned} \tag{18}$$

$$\mathfrak{G}_{1i}^T v_i - \mathfrak{U}\varsigma_{1,i} - \mathfrak{T}\varsigma_{2,i} < 0, \tag{19}$$

$$\mathbf{1}_n^T z_i - \mathfrak{V}(\mathbf{1}_r^T \mathfrak{G}_{3i}^T v_i)\mathbf{1}_n^T \varsigma_{4,i} < 0, \tag{20}$$

$$\mathfrak{G}_{2i}^T v_i + \mathfrak{H}_{1i}^T \mathbf{1} - \gamma \mathbf{1} < 0. \tag{21}$$

Furthermore, the sampled-data controller gain is $\mathscr{K}_i = \frac{z_i^T}{\mathbf{1}_r^T \mathfrak{G}_{3i}^T v_i}$

Proof Following the inequalities (13)-(16) in Theorem 2,

$$\mathfrak{G}_{0i}^T v_i + \rho v_i + \varsigma_{1,i} + \varsigma_{2,i} + \varsigma_{3,i} + \varsigma_{4,i}$$

$$+ \nu\varsigma_1 + \nu\varsigma_2 + \hbar\varsigma_3 + \hbar\varsigma_4 + \sum_{j=1}^{N} \pi_{ij} v_j + \mathfrak{H}_{0i}^T \mathbf{1} < 0, \tag{22}$$

$$\mathfrak{G}_{1i}^T v_i - \mathfrak{U}\varsigma_{1,i} - \mathfrak{T}\varsigma_{2,i} < 0, \tag{23}$$

$$\mathscr{K}_i^T \mathfrak{G}_{3i}^T v_i - \mathfrak{V}\varsigma_{4,i} < 0, \tag{24}$$

$$\mathfrak{G}_{2i}^T v_i + \mathfrak{H}_{1i}^T \mathbf{1} - \gamma \mathbf{1} < 0, \tag{25}$$

where

$$\begin{aligned} &\sum_{j=1}^{N} \pi_{ij}\varsigma_{1,j} \le \varsigma_1, \sum_{j=1}^{N} \pi_{ij}\varsigma_{2,j} \le \varsigma_2, \sum_{j=1}^{N} \pi_{ij}\varsigma_{3,j} \\ &\le \varsigma_3, \sum_{j=1}^{N} \pi_{ij}\varsigma_{4,j} \le \varsigma_4, \\ &\mathfrak{T} = e^{-\rho\nu}, \mathfrak{U} = (1-\nu_0)\mathfrak{T}, \mathfrak{V} = e^{-\rho\hbar}. \end{aligned} \tag{26}$$

Substituting $z_i = \mathscr{K}_i^T \mathfrak{G}_{3i}^T v_i$ into inequality (24) yields inequality (20). Moreover, inequalities (22) (23), and (25), together with constraint (26), which correspond exactly to inequalities (18), (19), and (21). Therefore, similar to the proof in Theorem 2, we can conclude that the positive system (3) under the sampled-data controller (2) is exponentially stable with $\mathscr{L}_1$-gain performance in mean.

Remark 5 In condition (20), the inequality $\mathbf{1}_n^T z_i - \mathfrak{V}(\mathbf{1}_r^T \mathfrak{G}_{3i}^T v_i)\mathbf{1}_n^T \varsigma_{4,i} < 0$ bounds the control effect in the Lyapunov analysis. Here, $z_i = \mathscr{K}_i^T \mathfrak{G}_{3i}^T v_i$, where $\mathscr{K}_i = \frac{z_i^T}{\mathbf{1}_r^T \mathfrak{G}_{3i}^T v_i}$, so $\mathfrak{G}_{3i}^T v_i$ is already embedded in the definition of z_i. The first term $\mathbf{1}_n^T z_i$ sums the components of z_i, representing the total control effect. The scaling factor $\mathbf{1}_r^T \mathfrak{G}_{3i}^T v_i$ appears in the second term because the bound on $\xi(t_k)$ (the sampled state) must account for the magnitude of the control effect across all input dimensions r, as defined by $\mathscr{K}_i$. This scaling arises from the Lyapunov derivation in Theorem 3, which extends condition (15) from Theorem 2 ($\mathbf{1}_n^T z_i \le V \mathbf{1}_n^T \varsigma_{4,i}$) by incorporating the sampled-data control $\hat{u}(t) = \mathscr{K}_i \xi(t_k)$. In this paper, since $r = 1$, $\mathbf{1}_r^T = 1$, simplifying $\mathbf{1}_r^T \mathfrak{G}_{3i}^T v_i$ to $\mathfrak{G}_{3i}^T v_i$.

4 Numerical evaluations

In this part of the article, we will show the usefulness of the theoretical findings by providing an example.

Example 1 Examine system (3), which has two subsystems and the system matrices shown below:

Mode 1:

$$\mathfrak{G}_{01} = \begin{bmatrix} -3 & 8 \\ 1 & -3 \end{bmatrix}, \quad \mathfrak{G}_{11} = \begin{bmatrix} 0.01 & 0.02 \\ 0.03 & 0.04 \end{bmatrix},$$

Table 2 Maximum allowable upper bound (MAUB) of ν for different values of $\hbar$ in Example 1

$\hbar$	0.05	0.10	0.15	0.2
ν	2.436	2.327	2.216	1.963

$$\mathfrak{G}_{21} = \begin{bmatrix} 0.1 \\ 0.1 \end{bmatrix}, \quad \mathfrak{G}_{31} = \begin{bmatrix} 0.1 \\ 0.1 \end{bmatrix},$$
$$\mathfrak{H}_{01} = [0.2, 0.3], \quad \mathfrak{H}_{11} = 0.4.$$

Mode 2:

$$\mathfrak{G}_{02} = \begin{bmatrix} -3 & 1 \\ 1 & -4 \end{bmatrix}, \quad \mathfrak{G}_{12} = \begin{bmatrix} 0.01 & 0.02 \\ 0.03 & 0.04 \end{bmatrix},$$
$$\mathfrak{G}_{22} = \begin{bmatrix} 0.2 \\ 0.1 \end{bmatrix}, \quad \mathfrak{G}_{32} = \begin{bmatrix} 0.2 \\ 0.1 \end{bmatrix},$$
$$\mathfrak{H}_{02} = [0.1, 0.2], \quad \mathfrak{H}_{12} = 0.2.$$

The transition rate matrix of the Markov process $\Upsilon(t)$ is taken as:

$$\Pi = \begin{bmatrix} -1 & 1 \\ 1 & -1 \end{bmatrix}.$$

By using the Linear Programming technique, setting $\nu = 0.6$; $\hbar = 0.1$; $\nu_0 = 0.3$; $\rho = 0.05$; $\gamma = 1$ and solving the condition (18)-(21), we have

$$v_1 = \begin{bmatrix} 0.2689 \\ 0.6838 \end{bmatrix}, \quad v_2 = \begin{bmatrix} 0.1543 \\ 0.2165 \end{bmatrix},$$
$$\varsigma_{11} = \begin{bmatrix} 3.6526 \times 10^{-10} \\ 6.8963 \times 10^{-10} \end{bmatrix}, \quad \varsigma_{12} = \begin{bmatrix} 2.5887 \times 10^{-10} \\ 3.9355 \times 10^{-10} \end{bmatrix},$$
$$\varsigma_{21} = \begin{bmatrix} 0.0239 \\ 0.0337 \end{bmatrix}, \quad \varsigma_{22} = \begin{bmatrix} 0.0239 \\ 0.0337 \end{bmatrix},$$
$$\varsigma_{31} = \begin{bmatrix} 7.0537 \times 10^{-11} \\ 1.3060 \times 10^{-10} \end{bmatrix}, \quad \varsigma_{32} = \begin{bmatrix} 1.2921 \times 10^{-10} \\ 1.7442 \times 10^{-10} \end{bmatrix},$$
$$\varsigma_{41} = \begin{bmatrix} 1.0741 \times 10^{-10} \\ 3.4189 \times 10^{-10} \end{bmatrix}, \quad \varsigma_{42} = \begin{bmatrix} 2.1405 \times 10^{-10} \\ 4.0133 \times 10^{-10} \end{bmatrix},$$
$$z_1 = \begin{bmatrix} 1.8623 \times 10^{-11} \\ 1.8623 \times 10^{-11} \end{bmatrix}, \quad z_2 = \begin{bmatrix} 9.7335 \times 10^{-12} \\ 9.7335 \times 10^{-12} \end{bmatrix},$$

The controller gain can be obtained from Theorem 3 as

$$\mathscr{K}_1 = \begin{bmatrix} 1.9548 \times 10^{-10} & 1.9548 \times 10^{-10} \end{bmatrix},$$
$$\mathscr{K}_2 = \begin{bmatrix} 1.8539 \times 10^{-10} & 1.8539 \times 10^{-10} \end{bmatrix}.$$

Figs. 1, 2, and 3 illustrate the dynamic behavior of the closed-loop system in Example 1 over the simulation

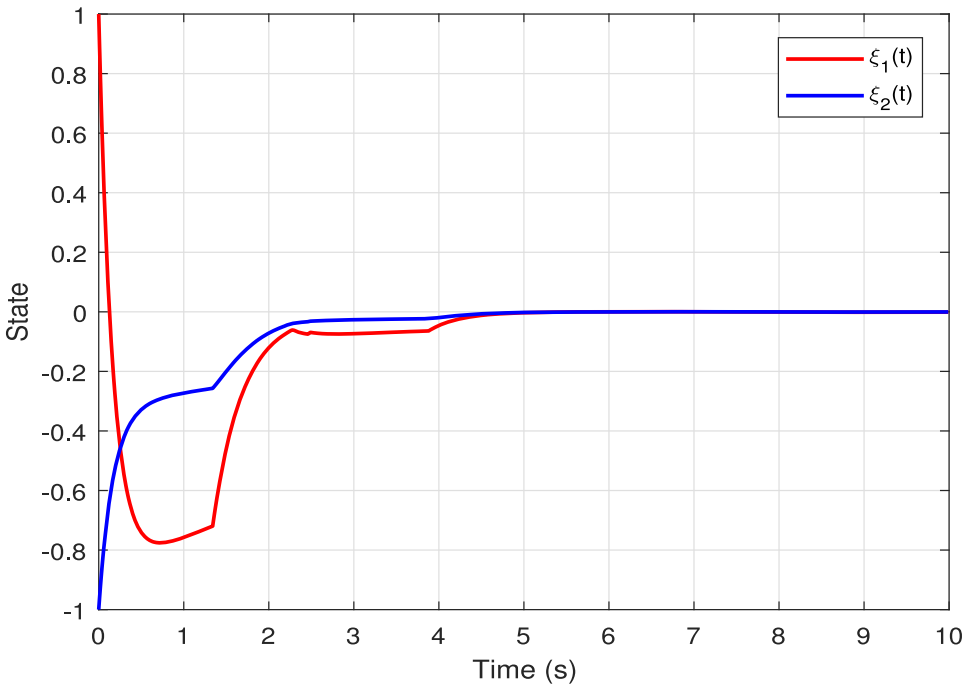

Fig. 1 State trajectory of the system (3) in Example 1

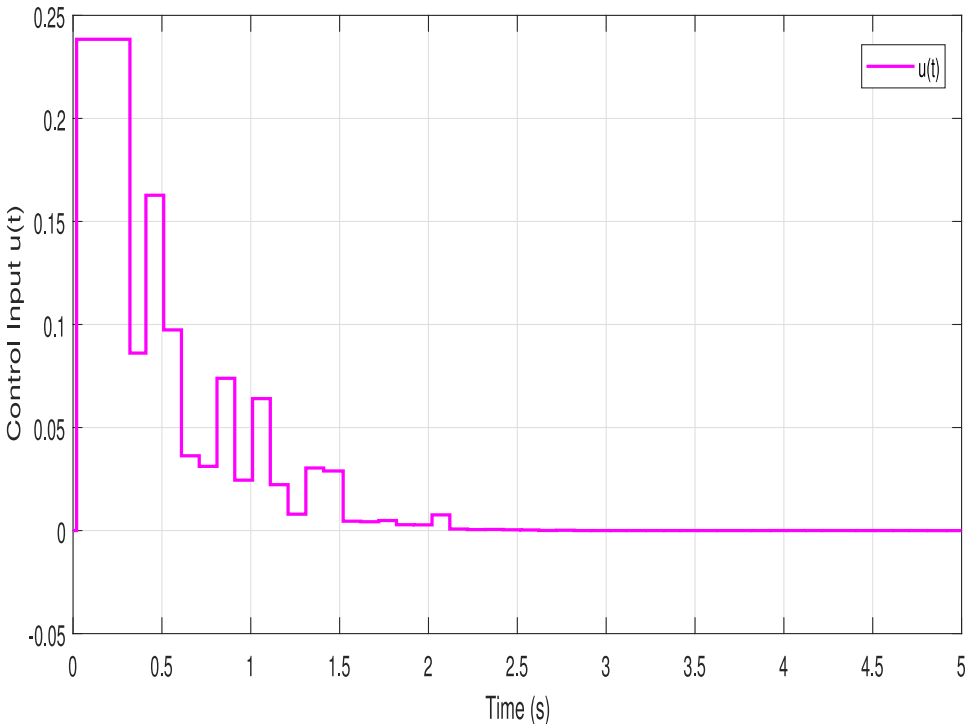

Fig. 2 Control responses of the system (3) in Example 1

period $t \in [0, 50]$. Figure 1, depicts the state trajectories $\xi(t) = [\xi_1(t), \xi_2(t)]^T$, which remain non-negative throughout, satisfying the positivity constraint of PMJSs. Both state components converge to zero exponentially, confirming the exponential stability in the mean as guaranteed by Theorem 1. The trajectories exhibit slight oscillations during mode switches, reflecting the influence of the disturbance $\hat{w}(t)$ and the Markovian transitions, but the $\mathscr{L}_1$-gain performance ($\gamma = 1$) ensures robustness against these perturbations. Figure 2, shows the control input $\hat{u}(t)$, which is piecewise constant due to the sampled-data control with a sampling period of $\hbar = 0.1$. The control magnitude is extremely small (on the order of 10^{-10}), consistent with the small controller gains $\mathscr{K}_1$ and $\mathscr{K}_2$, and it adjusts at each sampling instant and mode switch to stabilize the system. Figure 3 presents the Markovian mode $\Upsilon(t)$, which switches between Mode 1 and

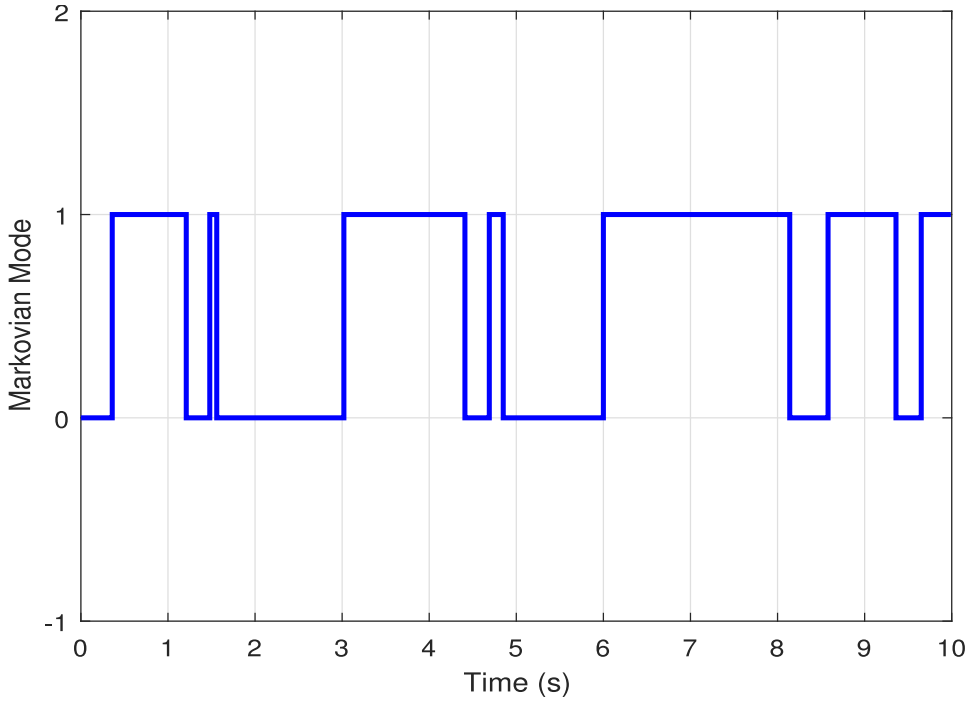

Fig. 3 Markovian modes of the system (3) in Example 1

Mode 2 with roughly equal frequency, as expected from the symmetric transition rates ($\pi_{12} = \pi_{21} = 1$). Table 2 represents the MAUB of ν for various values of $\hbar$. The frequent mode switches influence the state and control dynamics, but the designed controller effectively maintains stability and performance across both modes.

Example 2 Consider system (3) with two subsystems and the following system matrices:

Mode 1:

$$\mathfrak{G}_{01} = \begin{bmatrix} -2 & 0.1 & 0.05 \\ 0.2 & -1.5 & 0.1 \\ 0.1 & 0.05 & -1.8 \end{bmatrix}, \mathfrak{G}_{11} = \begin{bmatrix} 0.1 & 0.05 & 0.02 \\ 0.03 & 0.08 & 0.01 \\ 0.02 & 0.01 & 0.06 \end{bmatrix},$$

$$\mathfrak{G}_{21} = \begin{bmatrix} 0.1 \\ 0.2 \\ 0.15 \end{bmatrix}, \mathfrak{G}_{31} = \begin{bmatrix} 0.3 \\ 0.4 \\ 0.2 \end{bmatrix},$$

$$\mathscr{H}_{01} = \begin{bmatrix} 0.1 & 0.2 & 0.15 \end{bmatrix}, \mathscr{H}_{11} = 0.05,$$

Mode 2:

$$\mathfrak{G}_{02} = \begin{bmatrix} -1.8 & 0.15 & 0.08 \\ 0.25 & -1.2 & 0.12 \\ 0.1 & 0.07 & -1.6 \end{bmatrix}, \mathfrak{G}_{12} = \begin{bmatrix} 0.12 & 0.06 & 0.03 \\ 0.04 & 0.07 & 0.02 \\ 0.03 & 0.02 & 0.05 \end{bmatrix},$$

$$\mathfrak{G}_{22} = \begin{bmatrix} 0.15 \\ 0.25 \\ 0.1 \end{bmatrix}, \mathfrak{G}_{32} = \begin{bmatrix} 0.35 \\ 0.45 \\ 0.25 \end{bmatrix},$$

$$\mathscr{H}_{02} = \begin{bmatrix} 0.15 & 0.25 & 0.1 \end{bmatrix}, \mathscr{H}_{12} = 0.06,$$

The transition rate matrix of the Markov process $\Upsilon(t)$ is taken as:

$$\Pi = \begin{bmatrix} -0.9 & 0.9 \\ 0.1 & -0.1 \end{bmatrix}.$$

By using the Linear Programming technique, setting $\nu = 0.2$; $\hbar = 0.02$; $\nu_0 = 0.5$; $\rho = 0.01$; $\gamma = 0.5$ and solving the condition (18)-(21), we have

$$v_1 = \begin{bmatrix} 0.1024 \\ 0.1951 \\ 0.1020 \end{bmatrix}, \quad v_2 = \begin{bmatrix} 0.1405 \\ 0.2534 \\ 0.0987 \end{bmatrix},$$

$$\varsigma_{11} = \begin{bmatrix} 1.5642 \times 10^{-11} \\ 1.4042 \times 10^{-11} \\ 1.5713 \times 10^{-11} \end{bmatrix}, \quad \varsigma_{12} = \begin{bmatrix} 1.6100 \times 10^{-11} \\ 1.2715 \times 10^{-11} \\ 1.7244 \times 10^{-11} \end{bmatrix},$$

$$\varsigma_{21} = \begin{bmatrix} 0.0182 \\ 0.0218 \\ 0.0101 \end{bmatrix}, \quad \varsigma_{22} = \begin{bmatrix} 0.0300 \\ 0.0282 \\ 0.0142 \end{bmatrix},$$

$$\varsigma_{31} = \begin{bmatrix} 1.2660 \times 10^{-11} \\ 1.1422 \times 10^{-11} \\ 1.2488 \times 10^{-11} \end{bmatrix}, \quad \varsigma_{32} = \begin{bmatrix} 5.7769 \times 10^{-12} \\ 4.7131 \times 10^{-12} \\ 6.1278 \times 10^{-12} \end{bmatrix},$$

$$\varsigma_{41} = \begin{bmatrix} 2.2016 \times 10^{-10} \\ 4.9281 \times 10^{-11} \\ 1.0000 \times 10^{-6} \end{bmatrix}, \quad \varsigma_{42} = \begin{bmatrix} 2.2449 \times 10^{-10} \\ 2.7266 \times 10^{-11} \\ 1.0000 \times 10^{-6} \end{bmatrix},$$

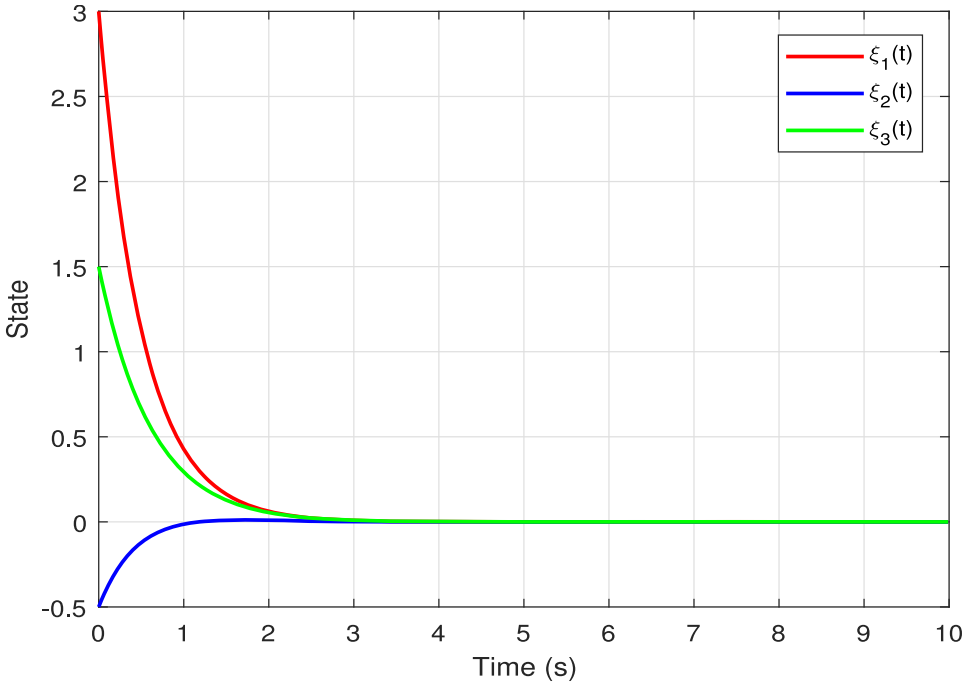

Fig. 4 State trajectory of the system (3) in Example 2

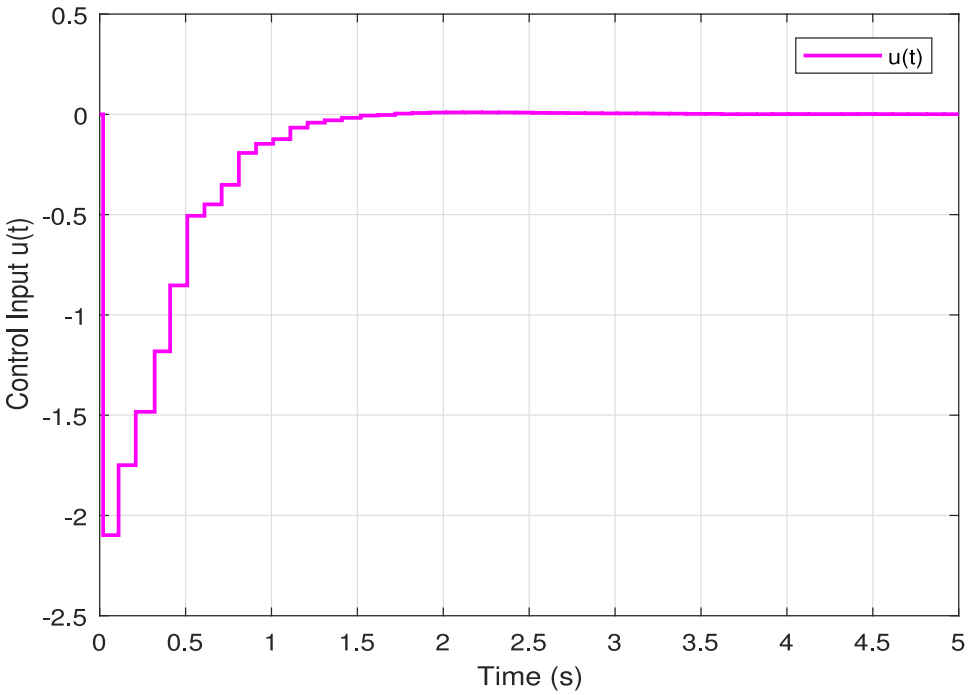

Fig. 5 Control responses of the system (3) in Example 2

$$z_1 = \begin{bmatrix} 5.1520 \times 10^{-11} \\ 5.1520 \times 10^{-11} \\ 5.1520 \times 10^{-11} \end{bmatrix}, \quad z_2 = \begin{bmatrix} 7.7370 \times 10^{-11} \\ 7.7370 \times 10^{-11} \\ 7.7370 \times 10^{-11} \end{bmatrix},$$

The controller gain can be obtained from Theorem 3 as

$$\mathscr{K}_1 = \begin{bmatrix} 3.9884 \times 10^{-10} & 3.9884 \times 10^{-10} & 3.9884 \times 10^{-10} \end{bmatrix},$$
$$\mathscr{K}_2 = \begin{bmatrix} 4.1179 \times 10^{-10} & 4.1179 \times 10^{-10} & 4.1179 \times 10^{-10} \end{bmatrix}.$$

Figs. 4, 5, and 6 provide a comprehensive view of the closed-loop system's behavior in Example 2 over $t \in [0, 50]$. Figure 4 illustrates the state trajectories $\xi(t) = [\xi_1(t), \xi_2(t), \xi_3(t)]^T$, which remain non-negative, adhering to the positivity property of PMJSs. All three state components converge to zero exponentially, validating the exponential stability in the mean established in Theorem 1. Compared to Example 1, the convergence appears smoother, likely due to the smaller sampling period ($\hbar = 0.02$) and

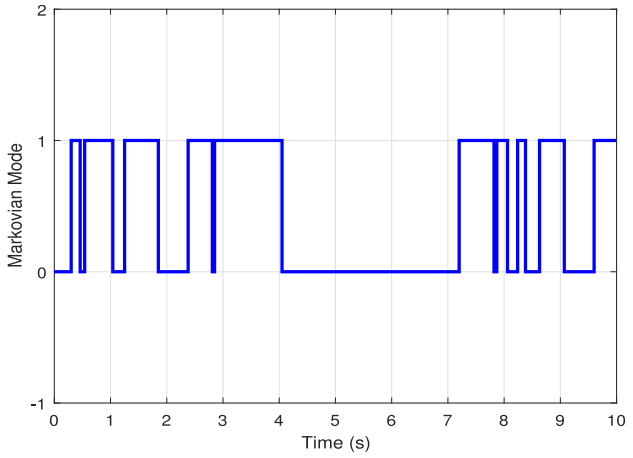

Fig. 6 Markovian modes of the system (3) in Example 2

the tighter $\mathscr{L}_1$-gain performance ($\gamma = 0.5$), which enhances disturbance attenuation against $\hat{w}(t)$. Figure 5 displays the control input $\hat{u}(t)$, which is piecewise constant with updates every $\hbar = 0.02$. The control magnitude remains small (on the order of 10^{-10}), reflecting the small controller gains, but it exhibits more frequent adjustments due to the reduced sampling period, ensuring precise stabilization across mode switches. Figure 6 shows the Markovian mode $\Upsilon(t)$, which predominantly resides in Mode 2, as expected from the transition rates ($\pi_{12} = 0.9, \pi_{21} = 0.1$). The system transitions to Mode 2 early in the simulation and remains there for longer periods, with occasional switches back to Mode 1, influencing the state and control dynamics. The controller effectively handles these asymmetric mode transitions, maintaining stability and achieving the desired $\mathscr{L}_1$-gain performance.

Remark 6 In the results of Example 1 and Example 2, the vectors $\mathscr{K}_1$ and $\mathscr{K}_2$ exhibit identical components within each mode. Specifically, in Example 1, $\mathscr{K}_1 = [1.9548 \times 10^{-10}, 1.9548 \times 10^{-10}]$, and in Example 2, $\mathscr{K}_1 = [3.9884 \times 10^{-10}, 3.9884 \times 10^{-10}, 3.9884 \times 10^{-10}]$, with similar patterns for $\mathscr{K}_2$. This behavior is a consequence of the alternating optimization approach. In the second optimization step, the constraint enforces condition (20), which requires $\mathbf{1}_n^T z_i - \mathfrak{V}(\mathbf{1}_r^T \mathfrak{G}_{3i}^T \upsilon_i)\mathbf{1}_n^T \varsigma_{4,i} < 0$, where $z_i = (\mathfrak{G}_{3i}^T \upsilon_i)\mathscr{K}_i^T$. Since $\mathscr{K}_i = [k_i, k_i, \ldots, k_i]$, this condition becomes $nk_i(\mathfrak{G}_{3i}^T \upsilon_i) - \mathfrak{V}(\mathbf{1}_r^T \mathfrak{G}_{3i}^T \upsilon_i)\mathbf{1}_n^T \varsigma_{4,i} < 0$. The constraint is symmetric with respect to the components of $\mathscr{K}_i$, as $\mathfrak{G}_{3i}^T \upsilon_i$ is a scalar. Additionally, the objective function minimizes sum($\mathscr{K}_1$) + sum($\mathscr{K}_2$), encouraging the smallest possible values for k_i. Since the constraint imposes no preference among the components of $\mathscr{K}_i$, the optimizer selects a solution where all components are equal, i.e., $\mathscr{K}_i = [k_i, k_i, \ldots, k_i]$, ensuring the minimal sum while satisfying the constraint. This symmetry explains the identical components observed in $\mathscr{K}_1$ and $\mathscr{K}_2$ across both examples.

Remark 7 It is noteworthy that in many industrial process, the dynamical behaviors are generally complex and nonlinear and their genuine mathematical models are always difficult to obtain. How to model the $\mathscr{L}_1$-gain stability analysis for Markov jump sampled-data control systems using a co-positive-type LKF approach has become one if the main theme in our research work. More particularly, some pioneering works have been done in the Makovian jump sampled-data system with a general LKF approach. The authors in [11] investigated nonlinear positive Markov jump systems with switching transition probabilities; however, it does not explicitly incorporate sampled-data control. Positive Markov jump systems under sampled-data control has been proposed in [17], but focuses solely on sampling-induced delay, modeled as $x(\tau(t))$, where $\tau(t)$ denotes the sampling delay, without accounting for additional inherent system time-varying delays. In contrast, our framework simultaneously addresses both the sampling-induced delay $\hbar(t)$ and the inherent system time-varying delay $\nu(t)$, making it applicable to systems in which delays originate from multiple sources, namely digital implementation (sampling) and physical system dynamics. In [24] studied switched positive T–S fuzzy systems with time-varying delays using a mode-dependent average dwell time approach, but does not consider a stochastic Markovian switching framework. This work stands out for its comprehensive integration of unique characteristics, such as positive system constraints, Markovian mode switching, sampled-data implementation, and dual time-varying delays (sampling-induced delay $\hbar(t)$ and system delay $\nu(t)$, $\mathscr{L}_1$-gain disturbance attenuation, and the presence of external disturbances $\hat{w}(t)$. The model considered in the present study is more practical than that proposed by [11],[17],[24], because they consider a usual Markovian Jump system with sampled data control via a general LKF approach based on stabilization conditions, but in this paper, we consider a new co-positive LKF approach with the combination of PMJSs via sampled-data control in the $\mathscr{L}_1$-gain performance. Henceforth, the investigation procedure and framework model proposed in this paper merit a lot of regard for fill such a demand all the more successfully

5 Conclusion

This study provides an in-depth exploration of exponential stability and $\mathscr{L}_1$-gain performance in PMJSs under sampled-data control. By incorporating sampled-data techniques, we have gained valuable insights into the stability and performance characteristics of these systems. We developed a sampled-data model for PMJSs and performed a thorough stability analysis, which served as the basis for our findings. The key contribution of this research is the application of sampled-data control to PMJSs, offering a robust theoretical framework and a systematic analysis methodology. This work advances the understanding of control systems

theory and provides practical implications for the design of sampled-data controllers in PMJSs. For future work, it would be beneficial to broaden the scope of these results by applying them to more complicated system structures or by integrating further performance metrics, which would increase the effectiveness and range of sampled-data control for PMJSs.

Data Availability No datasets were generated or analysed during the current study

Code Availability Not applicable.

References

1. Zhang W, Zhong S, Jiang X (2024) Finite-time annular domain stability and asynchronous H_∞ control for stochastic switching markov jump systems. IEEE Trans Autom Control 69:6277–6284
2. He H, Chen Y, Qi W, Wang M, Chen X (2022) Observer-based resilient control of positive systems with heterogeneous DoS attacks: a markov model approach. J Franklin Inst 359:272–293
3. Wang G, Ren Y (2022) Stability analysis of delayed markovian jump systems with delay switching and state signals and applications. Int J Robust Nonlinear Control 32:5141–5163
4. Mohanapriya S, Muthukumar P, Gopalakrishnan E, Gupta D (2025) Active disturbance reduction on non-homogeneous T-S fuzzy semi-Markovian jump systems and its application to secure digital signal communication. Chaos Solitons Fractals 196:116275
5. Gao C, Qi W, Cao J, Cheng J, Shi K (2025) Dynamic self-triggered control for positive fuzzy markov jump systems with switching transition rates. J Franklin Inst 362:107583
6. K Yin, D Yang, Y Tian, L Hu, (2025) Dynamic event-triggered $L1$ control of markov jump systems under positive constraint, communications in nonlinear science and numerical simulation. 109076
7. R Suresh, M Meiyanathan, R Vadivel, S Saravanan (2025) Exponential stability analysis of markovian jumping switched cellular neural networks via memory-event-triggered control. J Appl Math Comput 1–31
8. Chen G, Xia J, Park JH, Shen H, Zhuang G (2022) Asynchronous sampled-data controller design for switched markov jump systems and its applications. IEEE Trans Syst Man Cybern Syst 53:934–946
9. Yu X, Lin W (2024) Sampled-data feedback stabilization in mean square for stochastic homogeneous systems. IEEE Trans Autom Control 69:6805–6820
10. Yang J, Gao W (2024) Sampled-data control for T-S fuzzy systems using refined looped lyapunov functional approach. Symmetry 16:1119
11. Liu L-J, Xu N, Zhao X (2022) Stability and L_1-gain analysis of nonlinear positive markov jump systems based on a switching transition probability. ISA Trans 121:86–94
12. Qi W, Park JH, Cheng J, Kao Y, Gao X (2018) Exponential stability and L_1-gain analysis for positive time-delay markovian jump systems with switching transition rates subject to average dwell time. Inf Sci 424:224–234
13. Li S, Xiang Z, Karimi HR (2013) Stability and L_1-gain controller design for positive switched systems with mixed time-varying delays. Appl Math Comput 222:507–518
14. Zhao P, Kang Y, Niu B, Wang X (2022) Stochastic stability and stabilization of positive markov jump linear impulsive systems with time delay. IET Control Theory Appl 16:1731–1738
15. Lian J, Wang R (2021) Stochastic stability of positive markov jump linear systems with fixed dwell time. Nonlinear Anal Hybrid Syst 40:101014
16. Bhagyaraj T, Sabarathinam S, Popov V, Thamilmaran K, Vadivel R, Gunasekaran N (2023) Fuzzy sampled-data stabilization of hidden oscillations in a memristor-based dynamical system. Int J Bifurc Chaos 33:2350130
17. Zhao P, Niu B (2024) Exponential stability and L_1-gain performance for positive sampled-data control systems. Mathematics 13:110
18. Jin C-L, Wang Q-G, Wang R (2023) Exponential stability of sampled-data control systems with enhanced average sampling interval. Int J Control 96:1744–1753
19. Zhao X, Zhang L, Shi P, Liu M (2012) Stability of switched positive linear systems with average dwell time switching. Automatica 48:1132–1137
20. T Kaczorek (1998) Stabilization of positive linear systems, in: Proceedings of the 37th IEEE Conference on decision and control (Cat. No. 98CH36171). IEEE 1: 620–621
21. Zong G, Qi W, Karimi HR (2020) L_1 control of positive semi-markov jump systems with state delay. IEEE Trans Syst Man and Cybern Syst 51:7569–7578
22. Zhang J (2012) Sampled-data control of switched linear systems. pp 47–50
23. Xiang M, Xiang Z (2013) Stability, L_1-gain and control synthesis for positive switched systems with time-varying delay. Nonlinear Anal Hybrid Syst 9:9–17
24. Du S, Qiao J (2018) Stability analysis and L_1-gain controller synthesis of switched positive T-S fuzzy systems with time-varying delays. Neurocomputing 275:2616–2623
25. Ji Y, Chizeck HJ (1990) Controllability, stabilizability, and continuous-time markovian jump linear quadratic control. IEEE Trans Autom Control 35:777–788